Chem. Soc. **1991**, *113*, 3606–3607; c) Y. Diskin-Posner, S. Dahal, I. Goldberg, *Angew. Chem.* **2000**, *112*, 1344–1348; *Angew. Chem. Int. Ed.* **2000**, *39*, 1288–1292, and references therein; d) for infinite polyporphyrin assemblies that reveal distinct hollow structures, see C. V. K. Sharma, G. A. Brocker, J. G. Huddleston, J. W. Baldwin, R. M. Metzger, R. D. Rogers, *J. Am. Chem. Soc.* **1999**, *121*, 1137–1144.

[9] CSI-MS: a) S. Sakamoto, M. Fujita, K. Kim, K. Yamaguchi, *Tetrahedron* **2000**, *56*, 955; b) Y. Yamanoi, Y. Sakamoto, T. Kusukawa, M. Fujita, S. Sakamoto, K. Yamaguchi, *J. Am. Chem. Soc.* **2001**, *123*, 980–981.

[10] Using CH_3CN as the solvent enhanced the peak intensities in the CSI-MS study, probably because of its effective solvation of the cationic core which facilitated the separation of the PF_6^- counterions.

[11] For the determination of exact mass by CSI-MS, see K. Yamaguchi, S. Sakamoto, T. Imamoto, T. Ishikawa, *Anal. Sci.* **1999**, *15*, 1037–1038. The coordination number (m) of CH_3CN can be easily determined by using CD_3CN. For example, a 4^+ charged fragment at m/z 1051.3 was shifted to 1052.8 in CD_3CN. This corresponds to a 6 Da increase or to the coordination of two CD_3CN molecules in this fragment.

[12] A. K. Rappé, C. J. Casewit, K. S. Colwell, W. A. Goddard III, W. M. Skiff, *J. Am. Chem. Soc.* **1995**, *114*, 10024–10025.

[13] The assignment was confirmed by the disappearance of these peaks when [D_{10}]pyrene was used.

[14] CSI-MS data of the pyrene complex of $\mathbf{3}^{12+}\cdot 12NO_3^-$: CSI-MS ($CH_3CN/H_2O$ (1/1)) m/z: 1267.9 $[\mathbf{3}^{12+}-3NO_3^-+\text{pyrene}]^{3+}$, 935.4 $[\mathbf{3}^{12+}-4NO_3^-+\text{pyrene}]^{4+}$, 736.0 $[\mathbf{3}^{12+}-5NO_3^-+\text{pyrene}]^{5+}$, 603.3 $[\mathbf{3}^{12+}-6NO_3^-+\text{pyrene}]^{6+}$ (see the Supporting Information). Pyrene seems to be strongly entrapped within the cavity of $\mathbf{3}^{12+}$ since **3**–pyrene species were clearly observed by CSI-MS.

Preparation and Properties of Polymer-Wrapped Single-Walled Carbon Nanotubes**

Alexander Star, J. Fraser Stoddart,* David Steuerman, Mike Diehl, Akram Boukai, Eric W. Wong, Xin Yang, Sung-Wook Chung, Hyeon Choi, and James R. Heath*

Since the discovery[1] of single-walled carbon nanotubes (SWNTs) in 1993, it has become increasingly apparent that SWNTs, on account of their novel, structural, mechanical, and electronic properties, constitute a form of carbon with potential applications in many fields.[2] The remarkable electronic properties of SWNTs render them attractive candidates[2, 3] for use as the wiring components for nanoscale devices and circuitry. Many SWNT-based devices, such as field-effect transistors[3] and chemical sensors,[4] have been demonstrated. One major problem—from the standpoint of manipulating and processing SWNTs—is the insolubility of SWNTs in all solvents. Although considerable progress has been made on the open-end[5, 6] and side-wall[7] modifications of SWNTs using covalent chemistry, it has so far not been possible to establish an efficient means of handling and manipulating NTs without risking their partial destruction. Thus, it seems attractive to explore supramolecular approaches, that is, noncovalent modifications, since 1) they will not disrupt the extended π networks of SWNTs and 2) they could open up the possibilities of being able to organize NTs into ordered networks.

Molecules of high molecular weight that can either thread themselves onto or wrap themselves around the surfaces of SWNTs have attracted our attention as potential noncovalent modifiers of NTs that could disrupt the van der Waals interactions that cause SWNTs to aggregate into bundles. Polymers are appealing candidates to host the complexation of SWNTs since, given an appropriate structure, they can wrap themselves around SWNTs. Indeed, polymer–NT materials have been reported.[8] Composite materials based on conjugated luminescent polymers, such as poly(metaphenylenevinylene) (PmPV), filled with NTs exhibit[9] properties which are enhanced relative to those of the individual components. For example, NT/PmPV composites have exhibited nearly eightfold increases in electrical conductivity compared with just the polymer, and without impairment of the photo- and/or electroluminescence properties of the polymer.[9] Here we report on an efficient synthesis of a substituted PmPV, followed by the characterization of SWNT/PmPV′ complexes using UV/Vis and ^{1}H NMR spectroscopies. We then utilize AFM, optical, and electronic measurements of single, isolated SWNT/PmPV′ structures as a means to analyze quantitatively these systems.

Our preparation of the substituted PmPV[10] is summarized in Scheme 1. We have found that SWNTs can be suspended in solutions of PmPV′ in $CHCl_3$. The UV/Vis absorption spectra (Figure 1) were obtained from a dilute solution (0.06 mg mL^{-1}) of the polymer and the SWNT/PmPV′ complex in $CHCl_3$. Two major absorption bands were observed for PmPV′, with λ_{max} values of 329 and 410 nm. These bands broaden in the complex, presumably as a result of $\pi-\pi$ interactions between the SWNTs and the fully conjugated PmPV′ backbone. Moreover, the SWNT/PmPV′ complex yields a spectrum with broad absorptions around 650 and 900 nm. These wavelengths correspond roughly to the band-to-band transitions of pure SWNTs.[7c] While the polymer is bright yellow, the complex possesses a deep green color. The ^{1}H NMR (360 MHz, $CDCl_3$) spectrum of the SWNT/PmPV′ complex reveals (Figure 2a) significant broadening and small shifts in the resonances for the protons on the polymer, and even the TMS standard is broadened. This broadening arises most likely from the presence of conducting SWNTs, as well as from the presence of the ferromagnetic particles that are catalysts for the SWNT synthesis. Nevertheless, this broadening is not

[*] Prof. J. F. Stoddart, Prof. J. R. Heath, Dr. A. Star, D. Steuerman, M. Diehl, A. Boukai, Dr. E. W. Wong, Dr. X. Yang, S.-W. Chung, Dr. H. Choi
Department of Chemistry and Biochemistry
University of California, Los Angeles
405 Hilgard Avenue, Los Angeles, CA 90095-1569 (USA)
Fax: (+1) 310-206-1843
E-mail: stoddart@chem.ucla.edu, heath@chem.ucla.edu

[**] We would like to acknowledge the following agencies and foundations for supporting various aspects of this work: the polymer synthesis and spectroscopic characterization of the nanotube–polymer complex was funded by ONR; the chemical preparation and AFM analysis of these materials was supported by the NSF; device fabrication and charge-transport measurements were funded by DARPA and ONR; and the nonlinear microscopy experiments were supported by DARPA and the Keck Foundation.

Supporting information for this article is available on the WWW under http://www.angewandte.com or from the author.

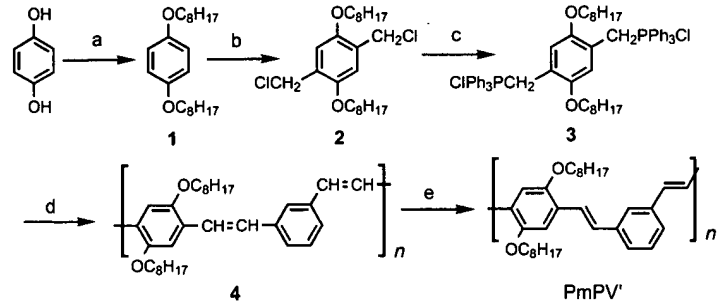

Scheme 1. The synthesis of PmPV'. a) $C_8H_{17}Cl$ (2 equiv), K_2CO_3, DMF, 90 °C, 71%; b) HCHO, HCl, dioxane/H_2O, 60–70 °C, 77%; c) Ph_3P (2 equiv), DMF, reflux, 83%; d) isophthaldehyde (1 equiv), NaOEt, EtOH/THF, 60%; e) I_2 (cat.), PhMe, reflux, 100%.

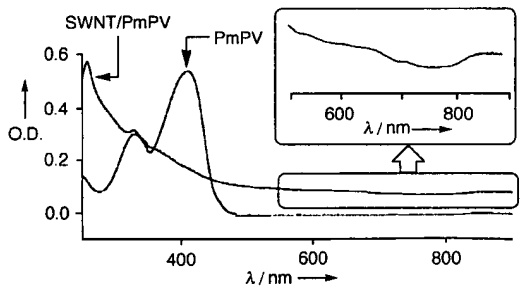

Figure 1. UV/Vis spectra (Cary 100 Bio, Varian, quartz cell) of PmPV' and the SWNT/PmPV' complex.

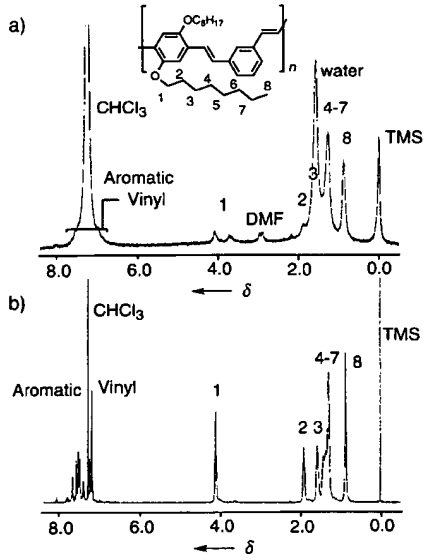

Figure 2. ^1H NMR spectra of a) the SWNT/PmPV' complex and b) PmPV' recorded in $CDCl_3$ (360 MHz).

completely uniform, which indicates that some chemical information is retained in the spectra of the SWNT/PmPV' complex. For example, the signals for the aromatic and vinyl protons on the PmPV' backbone, as well as the protons of the octyloxy chains that are closest to the aromatic groups, are the most broadened features. In addition, the peak intensities corresponding to the protons on the octyloxy chains that are closest to the aromatic rings are greatly reduced relative to those of the protons that are toward the middle or terminus of those chains. Similar phenomena have been observed previously[6b] when long alkyl chains were attached covalently to chemically modified SWNTs. All the spectroscopic evidence supports the notion that PmPV' wraps itself around the SWNTs, such that the phenylene rings and vinyl units that constitute the polymer backbone come close to the NTs' surfaces, presumably[11] as a result of $\pi-\pi$ interactions. Such an arrangement leaves the octyloxy chains attached to the polymer backbone able to wiggle around in solution.

Noncontact AFM images of the SWNT/PmPV' samples, investigated as a function of PmPV' concentration, also indicated that the polymer enters into significant noncovalent bonding interactions with the SWNTs. Three of these AFM images prepared from samples that were spin-coated onto mica wafers are shown in Figure 3. Nanotubes prepared from DMF solutions (Figure 3a) are characterized by regions of thick, aggregated SWNT ropes that have an average height of about 7.1 nm. The surface coverage of these SWNTs was inhomogeneous, with tubes localized only at isolated regions of the wafer. Well separated SWNT bundles are observed for the PmPV'/SWNT solutions (Figure 3b and c). The surface coverage becomes highly uniform as the polymer concentration increases. This apparent increase in coverage can be attributed to the polymer breaking up the ropes into suspensions of smaller ropes, and, indeed, the average diameter of the SWNT bundles decreases. At the lowest polymer concentrations studied the distribution of tube widths is broadened relative to the pure SWNT samples, but at higher concentrations this distribution narrows as the polymer breaks up the SWNT bundles into smaller diameter ropes (Table 1). For the highest polymer per nanotube concentration sample studied there is a large excess of polymer in solution. If it is assumed that all the tubes in this solution are single SWNT strands and that the polymer covers all the available area of the tubes there is still an approximately 50% excess of polymer molecules in solution. Nevertheless, even at this concentration, more polymer clearly helps disperse more tubes. The implication is that there is either an equilibrium between bound and excess polymer, or that excess of polymer is somehow needed to support SWNTs dispersed in $CHCl_3$.

When traditional characterization tools of UV/Vis and NMR spectroscopies are applied to SWNT/PmPV' solutions, the results are difficult to interpret and less informative than when they are applied to simpler systems. This situation arises from the heterogeneous character of the solution: it contains not just various diameters, lengths, and electrical types of tubes and ropes, but also both bound and free polymer. One way to avoid the problems associated with characterizing such a heterogeneous sample is to carry out measurements on single PmPV'-wrapped SWNT structures. In fact, both SWNTs and PmPV' have certain useful characteristics that can be exploited in the chemical analysis of the single structures. PmPV has uses[12, 13] as a photonic material: it can harvest light, and, when properly doped, PmPV devices can exhibit photovoltaic

  1433-7851/01/4009-1722 $ 17.50+.50/0 *Angew. Chem. Int. Ed.* **2001**, *40*, No. 9

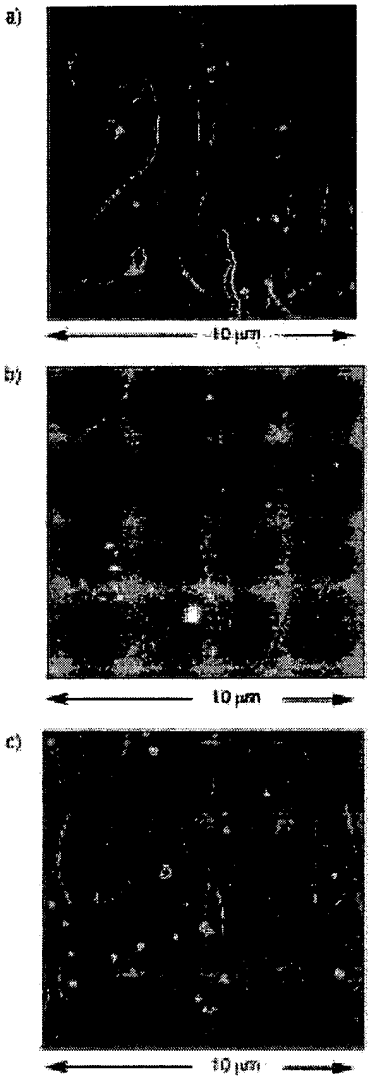

Figure 3. AFM images of bare and PmPV′-wrapped SWNTs: a) SWNTs prepared from 0.32 mg of SWNTs in 5 mL of DMF; b) solution containing 0.32 mg of SWNTs with 0.2 mg of PmPV′ in 5 mL of $CHCl_3$; c) solution containing 0.24 mg of SWNTs with 1 mg of PmPV′ in 5 mL of $CHCl_3$.

Table 1. Statistics of SWNT heights as determined by AFM images taken from samples with various polymer concentrations. The solution that contained no PmPV was DMF-based, while all the other solutions were $CHCl_3$-based.

SWNT [mg]	0.32	0.32	0.32	0.24
PmPV′ [mg]	0	0.2	0.6	1.0
average diameter [nm]	7.1	6.0	5.8	3.4
standard deviation	3.9	4.7	4.0	2.4

responses. In addition, PmPV′ also has distinctive UV/Vis absorption and fluorescence spectra. Finally, the high aspect ratio of SWNTs that makes them relatively easy to locate and image using AFM, also makes them ideal candidates for bridging across electrodes for charge-transport measurements. Hence, we conclude our discussion here by describing two more experiments: 1) the photoconductivity response of a single polymer-wrapped SWNT bundle and 2) two-photon fluorescence (2PF) measurements of single SWNT/PmPV′ bundles, correlated with AFM structural measurements. These experiments indicate that the polymer is, in fact, in intimate electrical contact with the NTs, and that the polymer wraps around bundles of tubes, rather than wrapping around individual tubes which then aggregate to form ropes. Although neither experiment explicitly interrogates the extent of the PmPV′ wrapping, the results of both experiments are consistent with at least a high level, if not complete, coverage of the SWNT bundle by the PmPV′.

SWNT/PmPV′ photovoltaic devices were fabricated by spin coating a dilute solution of polymer-coated SWNTs in $CHCl_3$ onto a silica substrate that was pre-patterned with Au microelectrodes (200 nm diameter widths and 1 μm electrode spacing). AFM measurements revealed that a single SWNT bundle bridged the two electrodes. This device was mounted onto the cold finger of an immersion cryostat equipped with optical access ports. Filtered light from a quartz-halogen lamp was directed through a monochromator and then onto the device. A small bias was applied and the photoresponse of the device was measured by cycling the light. Such measurements were carried out as a function of temperature, wavelength, and applied bias. Control experiments on unwrapped SWNT devices yielded no photodependent response. The photoresponse of a SWNT/PmPV′ device at 375 nm excitation is shown in Figure 4. If we correlate the photoinduced current

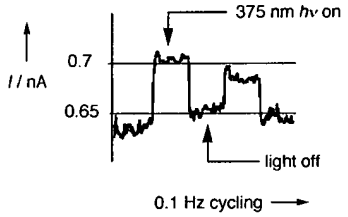

Figure 4. The performance of a PmPV′-wrapped SWNT photovoltaic device measured at 10 K. The excitation wavelength was 375 nm (slightly less than 1 mW focused to 0.2 cm^2, with a device area of approximately 5×10^{-11} cm^2), and a +0.025 V bias was applied to the device. Room temperature yielded a similar response if a +0.005 V bias was applied.

increase (ca. 4×10^8 $e\,s^{-1}$) with the photon flux onto the SWNT/PmPV′ structure (7×10^5 photons s^{-1}) we find that the polymer is not harvesting the light, but rather the photoexcited polymer is "gating" the SWNT device, and so the signal from an absorbed photon is greatly amplified. This means that the polymer, in the exited state, has a dipole moment that alters the local electric field at the surface of the SWNT bundle. It was possible, by measuring the photoinduced increase in current through the tube as a function of excitation wavelength, to map out the absorption spectrum of the polymer. The critical result here is that these measurements do indicate that the polymer is in intimate electrical contact with the SWNT bundle.

Optical experiments, correlated with structural measurements, were also carried out on single PmPV′-wrapped SWNTs and used to interrogate the general morphology of

the SWNT/PmPV′ structure. To this end, we have correlated the two-photon fluorescence (2PF) intensity with the diameter of various SWNT/PmPV′ structures. Unwrapped SWNT ropes exhibited no 2PF signal. Silica substrates were prepatterned with micron-sized gold alignment markers, and dilute SWNT/PmPV′ solutions were deposited onto the wafer by spin coating. AFM analysis revealed both SWNT structures and polymer particles, but the polymer particles could be removed selectively by exhaustive washing with $CHCl_3$. The positions of the SWNT/PmPV′ structures were recorded with respect to alignment markers (Figure 5a) using noncontact AFM. Such measurements also yielded the height (diameter) of the SWNT bundles at various positions along their length. The wafers were then mounted onto the illumination stage of a custom built, scanning nonlinear optical microscope capable of approximately 1 μm^2 spatial resolution.[14] Both 2PF images and second harmonic generation (SHG) images were simultaneously recorded, while various filters, polarizers, and beam splitters were employed to isolate the two signals at separate detectors. Both images were utilized. The alignment markers were detected by SHG, and the SWNT/PmPV′ structures were detected by 2PF (Figure 5b). We correlated the diameter of a SWNT structure with the magnitude of the 2PF signal for a number of SWNT/PmPV′ structures from both the AFM and the 2PF measurements (Figure 5c). These data distinguish between the two polymer-wrapping possibilities. If the individual SWNT strands within a bundle are wrapped, then the 2PF signal from the bundle should scale as the square of the bundle diameter, since the volume of the bundle is effectively filled with PmPV′. However, if the polymer just wraps around the surface of the bundle, then the 2PF signal should scale linearly with the bundle diameter. It is clear from Figure 5c that the scaling is linear, and hence that the polymer wraps around the already aggregated bundle.

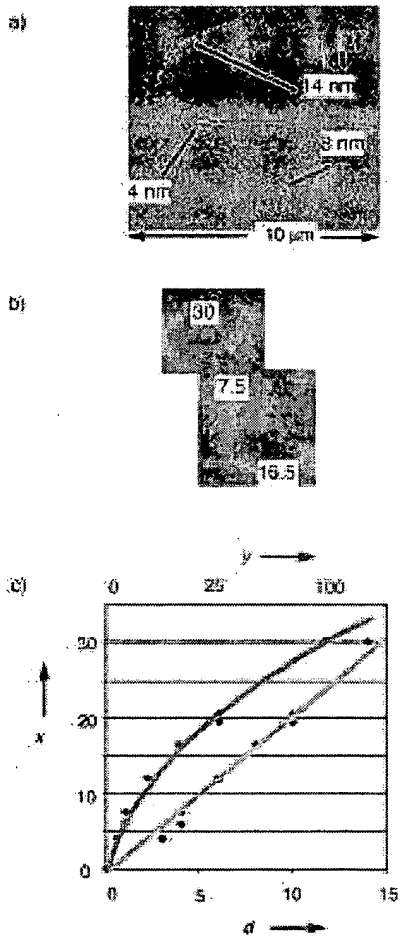

Figure 5. a) Atomic force micrograph of a polymer-wrapped SWNT bundle. The diameter of the SWNT varies in the three significant sections labeled in the image. At the top right of the image is an alignment marker. b) 2PF image of the same SWNT with the various signal strengths (relative to background) of the fluorescence signal indicated. c) A correlation of the two plots (and other similar data) presented in two ways. The blue curve represents the fluorescence intensity plotted against the diameter of the SWNT bundle while the red curve is the fluorescence intensity plotted versus the square of the radius of the SWNT bundle. Only the blue curve is linear, which indicates that the PmPV wraps only around the exterior of the SWNT bundle, and that PmPV-wrapped SWNT structures do not further aggregate to form larger diameter ropes. (x: 2PF signal; d: diameter of the SWNT bundle; y: (bundle diameter)^2).

This last issue is important in the context of using polymers as a chemical means of separating the various different SWNT types. Finally, returning to our initial motivation, the experiments reported here do indicate that the electrical properties of SWNTs are largely unperturbed by the associated polymer. It appears that PmPV may provide a useful route toward "functionalizing" the SWNTs without destroying their electrical character.

Experimental Section

PmPV′: The synthesis of the polymer **4** was achieved in five steps starting from hydroquinone, which is O-alkylated with octyl chloride and K_2CO_3 in DMF at 90 °C. The resulting 1,4-bis(octyloxybenzene) (**1**) was chloromethylated with HCl and HCHO in dioxane/water at 60–70 °C. The resulting 1,4-bis(chloromethyl)-2,5-dioctyloxybenzene (**2**) was then heated under reflux with PPh_3 in DMF. Multiple Wittig condensations were used to polymerize the resulting bis(triphenylphosphonium salt) **3** with isophthaldehyde using NaOEt in dry EtOH/THF to afford a polymer **4**, which was converted into its pure *trans* isomer (PmPV) by refluxing in PhMe in the presence of a catalytic amount of I_2. The polymerization reaction under different conditions produces both low and high molecular weight polymers. The molecular weights of the polymers were determined as 9200 and 150000 in THF by using size-exclusion chromatography (SEC). The SEC system was calibrated by using polystyrene standards prior to use. Low molecular weight polymer: ^{1}H NMR (360 MHz, $CDCl_3$): $\delta = 7.64$ (s, 1H), 7.50 (m, 4H), 7.37 (t, $J = 7.5$ Hz, 1H), 7.21 (s, 1H), 7.16 (s, 3H), 4.09 (t, $J = 6.5$ Hz, 2H), 1.90 (p, $J = 6.5$ Hz, 2H), 1.55 (p, $J = 6.5$ Hz, 2H), 1.35 (m, 8H), 0.87 (t, $J = 6.5$ Hz, 3H); ^{13}C NMR (90 MHz, $CDCl_3$): $\delta = 151.0$, 138.3, 128.5, 126.9, 125.7, 124.0, 111.1, 69.8, 31.8, 29.4, 26.3, 22.7, 14.1.

Preparation of the SWNT/PmPV′ complex for spectroscopic analysis: The SWNTs were obtained as a surfactant-stabilized water suspension (from Tubes@Rice). The nanotube sheets were typically made by vacuum filtration of around 1.5 mL of an approximately 4 mg mL^{-1} nanotube suspension through a poly(tetrafluoroethylene) filter (Gelman, 25 mm in diameter, 0.2 μm pores). The nanotube sheet (formed over the clear funnel area, which was 15 mm in diameter) was washed with deionized water (5 mL) and then MeOH (5 mL) to remove residual NaOH and surfactant, respectively. These sheets were allowed to dry under vacuum at room temperature overnight before being peeled from the filter. The typical nanotube sheet weighed about 6 mg. It was then resuspended by sonication (2.5 h) in DMF in a water bath (Branson model 1510, 40 kHz). The DMF

  1433-7851/01/4009-1724 $ 17.50+.50/0 *Angew. Chem. Int. Ed.* **2001**, *40*, No. 9

was then removed by high vacuum and a chloroform solution of polymer PmPV' was added (5 mg in 5 mL). Sonication for 2 h gave a stable suspension that was filtered prior to spectroscopy.

Preparation of the SWNT/PmPV' material prior to AFM: Aliquots of Triton X-100 SWNTs (from Tubes@Rice) were purified by centrifugation at 14000 rpm in MeOH. The purified tubes were re-suspended in fresh MeOH by shaking, and then they were vacuum filtered over a 0.2 mm PTFE filter and washed with MeOH and 18 MQ H_2O to form a nanotube mat. A portion of the mat weighing 6–7 mg was sonicated in DMF using a bath sonicator while stepwise adding the DMF until a total volume of 25 mL was obtained. The DMF/NT stock solution was sonicated for a period of 6 h. Measured aliquots of the stock solution were transferred to round-bottom flasks and the DMF was removed by rotary evaporation. Each flask contained between 0.24–0.32 mg of SWNTs. 5 mL of $CHCl_3$ containing between 0.2–1.0 mg of dissolved PmPV were added to these flasks. The SWNT/PmPV' mixtures were sonicated for 15 mins. After sonication, one drop of the SWNT/PmPV' solution was placed on a freshly cleaved 1 cm^2 mica wafer, and subsequently washed with 5 drops of $CHCl_3$ while spinning it at 750 rpm to wash off the excess of the polymer. AFM images were collected in noncontact mode.

Received: December 18, 2000 [Z16297]

[1] S. Ijima, T. Ichihashi, *Nature* **1993**, *363*, 603–605.

[2] P. M. Ajayan, *Chem. Rev.* **1999**, *99*, 1787–1799.

[3] a) S. J. Tans, C. Dekker, *Nature* **2000**, *404*, 834–835; b) S. J. Tans, A. R. M. Verschueren, C. Dekker, *Nature* **1998**, *393*, 49–52; c) S. J. Tans, M. H. Devoret, H. Dai, A. Thess, R. E. Smalley, L. J. Geerligs, C. Dekker, *Nature* **1997**, *386*, 474–477.

[4] J. Kong, N. R. Franklin, C. Zhou, M. G. Chapline, S. Peng, K. Cho, H. Dai, *Science* **2000**, *287*, 622–625.

[5] J. Liu, A. G. Rinzler, H. Dai, J. H. Hafner, R. K. Bradley, P. J. Boul, A. Lu, T. Iverson, K. Shelimov, C. B. Huffman, F. Rodriguez-Macias, Y.-S. Shon, T. R. Lee, D. T. Colbert, R. E. Smalley, *Science* **1998**, *280*, 1253–1256.

[6] a) J. Chen, M. A. Hamon, H. Hu, Y. Chen, A. M. Rao, P. C. Eklund, R. C. Haddon, *Science* **1998**, *282*, 95–98; b) M. A. Hamon, J. Chen, H. Hu, Y. Chen, M. E. Itkis, A. M. Rao, P. C. Eklund, R. C. Haddon, *Adv. Mater.* **1999**, *11*, 834–840; c) J. E. Riggs, Z. Guo, D. L. Carroll, Y.-P. Sun, *J. Am. Chem. Soc.* **2000**, *122*, 5879–5880.

[7] a) E. T. Mickelson, C. B. Huffman, A. G. Rinzler, R. E. Smalley, R. H. Hauge, J. L. Margave, *Chem. Phys. Lett.* **1998**, *296*, 188–194; b) E. T. Mickelson, I. W. Chiang, J. L. Zimmerman, P. J. Boul, J. Lozano, J. Liu, R. E. Smalley, R. H. Hauge, J. L. Margrave, *J. Phys. Chem. B* **1999**, *103*, 4318–4322; c) P. J. Boul, J. Liu, E. T. Mickelson, C. B. Huffman, L. M. Ericson, I. W. Chiang, K. A. Smith, D. T. Colbert, R. H. Hauge, J. L. Margrave, R. E. Smalley, *Chem. Phys. Lett.* **1999**, *310*, 367–372.

[8] Polymers that have been used to prepare composites with SWNTs include polymethylmethacrylate, see: a) M. Yudasaka, M. Zhang, C. Jabs, S. Ijima, *Appl. Phys. A* **2000**, *71*, 449–451; b) C. Stephan, T. P. Nguyen, M. Lamy de la Chapelle, S. Lefrant, C. Journet, P. Bernier, *Synth. Met.* **2000**, *108*, 139–149. Polymers have also been used to prepare composites with multi-walled nanotubes, see: c) M. S. P. Shaffer, A. H. Windle, *Adv. Mater.* **1999**, *11*, 937–941; d) Z. Jin, X. Sun, G. Xu, S. H. Goh, W. Ji, *Chem. Phys. Lett.* **2000**, *318*, 505–510. Recently, polymers have been used in the spinning of SWNTs into long fibers, see: e) B. Vigolo, A. Penicaud, C. Coulon, C. Sauder, R. Pailler, C. Journet, P. Bernier, P. Poulin, *Science* **2000**, *290*, 1331–1334.

[9] a) S. A. Curran, P. M. Ajayan, W. J. Blau, D. L. Carroll, J. N. Coleman, A. B. Dalton, A. P. Davey, A. Drury, B. McCarthy, S. Maier, A. Strevens, *Adv. Mater.* **1998**, *10*, 1091–1093; b) S. Curran, A. P. Davey, J. N. Coleman, A. B. Dalton, B. McCarthy, S. Maier, A. Drury, D. Gray, M. Brennan, K. Ryder, M. Lamy de la Chapelle, C. Journet, P. Bernier, H. J. Byrne, D. Carroll, P. M. Ajayan, S. Lefrant, W. Blau, *Synth. Met.* **1999**, *103*, 2559–2562; c) J. N. Coleman, A. B. Dalton, S. Curran, A. Rubio, A. P. Davey, A. Drury, B. McCarthy, B. Lahr, P. M. Ajayan, S. Roth, R. C. Barklie, W. J. Blau, *Adv. Mater.* **2000**, *12*, 213–216.

[10] a) A. P. Davey, A. Drury, S. Maier, H. J. Byrne, W. J. Blau, *Synth. Met.* **1999**, *103*, 2478–2479; b) O. Toshihiro, N. Takanobu, D. Shuji (Sumitomo Chemical Co), EP0901174, **1999** [*Chem. Abstr.* **1999**, *139*, 202731c]; c) Y. Pang, J. Li, B. Hu, F. E. Karasz, *Macromolecules* **1999**, *32*, 3946–3950.

[11] Computer modeling (molecular mechanics and molecular dynamics simulations) has been carried out by us to probe the nature of the interaction between a short (10,10)-SWNT and a PmPV' of eight repeating units. These calculations support a model in which the polymer is wrapped helically around the nanotubes with the phenylene rings in the polymer backbone stacked in a "face-to-face" manner against the walls of the nanotube. For another recent example of calculations carried on the binding of different polymers to carbon nanotubes, see V. Lordi, N. Yao, *J. Mater. Res.* **2000**, *15*, 2770–2779.

[12] For an early report on polymeric light-emitting diodes (LEDs) based on poly(paraphenylenevinylene) (PPV), see J. H. Burroughes, D. D. C. Bradley, A. R. Brown, R. N. Marks, K. Mackay, R. H. Friend, P. L. Burns, A. B. Holmes, *Nature* **1990**, *347*, 539–541.

[13] For an excellent review on electroluminescent conjugated polymers, see A. Kraft, A. C. Grimsdale, A. B. Holmes, *Angew. Chem.* **1998**, *110*, 416–443; *Angew. Chem. Int. Ed.* **1998**, *37*, 402–428.

[14] S. Henrichs, J. Sample, J. Shiang, C. P. Collier, R. J. Saykally, J. R. Heath, *J. Phys. Chem. B* **1999**, *103*, 3524–3528.

T_h-Symmetric Nanoporous Network Built of Hexameric Metallamacrocycles with Disparate Cavities for Guest Inclusion**

Cheng-Yong Su, Xiao-Ping Yang, Bei-Sheng Kang,* and Thomas C. W. Mak*

Growing interest in the rational design and construction of nanoporous structures[1] is motivated principally by the potential exploitation of the resulting cavities and channels in nanotechnology, including shape- and size-selective catalysis, molecular recognition, ion exchange, separation, and optoelectronic applications.[2] Rapid growth and breakthroughs in this field rely on, to a large degree, mastery of the novel synthetic protocol in the construction of organized supramolecular systems, namely self-assembly of multiple building blocks in a single step into large aggregates of molecules through noncovalent interactions.[3] On the other hand, difficulties were often encountered in the generation of porous networks, such as the control of cavity size and geometry, the prevention of network interpenetration, and

[*] Prof. B.-S. Kang, Dr. C.-Y. Su, X.-P. Yang
School of Chemistry and Chemical Engineering
Zhongshan University
Guangzhou 510275 (PR China)
Fax: (+86) 20-84110318
E-mail: cesscy@zsu.edu.cn
Prof. T. C. W. Mak
Department of Chemistry
The Chinese University of Hong Kong
Shatin, New Territories, Hong Kong SAR (PR China)
Fax: (+852) 26035057
E-mail: tcwmak@cuhk.edu.hk

[**] This work is supported by the National Natural Science Foundation of China, the Natural Science Foundation of Guangdong Province and Hong Kong Research Grants Council Earmarked Grant CUHK 4206/99P.